IRIS AperTO

UNIVERSITÀ DEGLI STUDI DI TORINO

AperTO - Archivio Istituzionale Open Access dell'Università di Torino

Heterozygous PNPT1 variants cause spinocerebellar ataxia type 25

This is a pre print version of the following article:

Original Citation:

Availability:

This version is available http://hdl.handle.net/2318/1854166 since 2022-06-20T13:57:44Z

Published version:

DOI:10.1002/ana.26366

Terms of use:

Open Access

Anyone can freely access the full text of works made available as "Open Access". Works made available under a Creative Commons license can be used according to the terms and conditions of said license. Use of all other works requires consent of the right holder (author or publisher) if not exempted from copyright protection by the applicable law.

(Article begins on next page)

25 September 2024

Heterozygous loss of function of *PNPT1* accounts for sensory and cerebellar ataxia in spinocerebellar ataxia type 25

Authors

Mathieu Barbier[1]*, Melanie Bahlo[2,3]*, Alessandra Pennisi[4,5], Maxime Jacoupy[1], Rick M Tankard[2,3], Claire Ewenczyk[1], Kayli C Davies[6,7], Patricia Lino-Coulon[1], Claire Colace[1], Haloom Rafehi[2,3], Nicolas Auger[1], Brendan Ansell[2,3], Ivo van der Stelt[2,3], Katherine B Howell[7,8,9], Marie Coutelier[1], David J Amor[7,9], Emeline Mundwiller[1], Lena Guillot-Noël[1], Elsdon Storey[10], R J McKinlay Gardner[11], Mathew J Wallis[12], Alfredo Brusco[13], Olga Corti[1], Agnès Rötig[4,5], Richard J Leventer[7,8,9], Alexis Brice[1], Martin B Delatycki[6,7,14], Giovanni Stevanin[1]**, Paul J Lockhart[6,7]**[#] and Alexandra Durr[1]**[#].

Affiliations

[1]Sorbonne Université, Institut du Cerveau - Paris Brain Institute - ICM, Inserm, CNRS, APHP, Hôpital de la Pitié Salpêtrière, Paris, France.

[2]Population Health and Immunity Division, The Walter and Eliza Hall Institute of Medical Research, Melbourne, Victoria 3052, Australia.

[3]Department of Medical Biology, University of Melbourne, Melbourne, Victoria 3010, Australia.

[4]Necker Hospital, APHP, Reference Center for Mitochondrial Diseases, Genetics Department, Institut Imagine, University of Paris, Paris, France.

[5]Inserm UMR_S1163, Institut Imagine, Paris, France.

[6]Bruce Lefroy Centre, Murdoch Children's Research Institute, Melbourne, Victoria 3052, Australia.

[7]Department of Paediatrics, University of Melbourne, Melbourne, Victoria 3010, Australia.

[8]Department of Neurology, Royal Children's Hospital, Melbourne, Victoria 3052, Australia.

[9]Murdoch Children's Research Institute, Melbourne, Victoria 3052, Australia.

[10]School of Public Health and Preventive Medicine, Monash University, Melbourne, Victoria 3004, Australia.

[11]Clinical Genetics Group, University of Otago, Dunedin 9016, New Zealand.

[12]Clinical Genetics Service, Austin Health, Melbourne, Australia; Department of Medicine, University of Melbourne, Austin Health, Melbourne, Australia.

[13]Department of Medical Sciences, University of Torino, Torino, Italy.

[14]Victorian Clinical Genetics Service, Melbourne 3052, Australia

* These authors contributed equally.

** Joint senior authors

[#] **Corresponding Authors**

Pr. Alexandra Durr, MD, PHD, Paris Brain Institute, Hopital Pitié-Salpêtrière, 47, boulevard de l'Hôpital CS21414, 75646 PARIS CEDEX 13 ; mail : alexandra.durr@icm-institute.org

Pr. Paul Lockhart, PHD, Bruce Lefroy Centre, Murdoch Children's Research Institute, Melbourne, Victoria 3052, Australia, mail : paul.lockhart@mcri.edu.au

Summary

Dominant spinocerebellar ataxias (SCA) are characterized by genetic heterogeneity. Some mapped and named *loci* remain without a causal gene identified. Whole-exome and whole-genome sequencing were performed in the French family in which the SCA25 *locus* was previously mapped. A heterozygous pathogenic variant causing exon skipping was identified in the gene encoding Polyribonucleotide Nucleotidyltransferase PNPase 1 (*PNPT1)* located in the SCA25 linkage interval. A second splice variant in *PNPT1* was detected in a large Australian family with a dominant ataxia also mapping to SCA25. An additional nonsense variant was detected in an unrelated individual with ataxia. The phenotype spans slowly evolving sensory and cerebellar ataxia, in some cases attributed to ganglionopathy. Both nonsense and splice heterozygous variants result in premature stop codons, and lead to haploinsufficiency at the protein level. In addition, an elevated type I interferon response was observed in blood from all affected heterozygous carriers tested compared to those with wildtype *PNPT1*. PNPase is involved in mitochondrial RNA (mtRNA) processing and prevents the abnormal accumulation of double-stranded mtRNAs in the mitochondria and leakage into the cytoplasm, associated with triggering a type I interferon response. In conclusion, this study identifies *PNPT1* as a new SCA gene, responsible for SCA25, and highlights biological links between alterations of mtRNA trafficking, interferonopathies and ataxia.

Keywords: spinocerebellar ataxia; sensory neuropathy, SCA25; *PNPT1*; type I interferon response.

Spinocerebellar ataxias (SCA) are a heterogeneous group of autosomal dominant neurodegenerative disorders. Variable clinical presentations mostly include cerebellar ataxia manifesting as gait disturbance, incoordination of upper limb movements, nystagmus and dysarthria, with additional pyramidal or extrapyramidal features. A non-exhaustive list of other symptoms that can be associated with SCA includes peripheral neuropathy, cognitive impairment, dystonia, Parkinsonism and hearing loss. Variable age at onset is observed between and among SCA subtypes. Genetic heterogeneity is also a hallmark of SCA with 48 SCA *loci* described so far. We previously mapped the SCA25 *locus* (MIM: 608703) in a French family in which cerebellar ataxia and prominent sensory neuropathy segregated as an autosomal dominant trait[1]. Both age at onset and severity of the disease were highly variable. Two relatives with the SCA25 haplotype were unaffected or very mildly affected, showing either incomplete penetrance or very late onset. At that time, the size of the region of interest and the high number of genes located in the chromosomal interval precluded the identification of the causal variant.

Whole Exome Sequencing (WES) was performed in five individuals, four affected and one spouse (non-carrier) in this family (Figure 1A and Table 1). The index case was first seen at age 22 yrs. Onset was at 1 year of age. He was not able to run at age 3 yrs. and had frequent vomiting during childhood. A clinical diagnosis of Friedreich ataxia was made at age 8 yrs., but no *FXN* expansion was found. He required a wheelchair for mobility from age 13 yrs. He was found to have a predominantly sensory neuropathy. He had moderate dysarthria and flexor plantar responses and was of normal intelligence. Ocular movement recordings showed square waves, hypermetric saccades, and gaze evoked nystagmus. Examination at age 32 yrs. was notable for the presence of chronic cough, generalized wasting with abolished vibration sense and decreased sensitivity to touch and pinprick distally. MRI showed severe cerebellar atrophy involving the vermis and hemispheres, as well as the bulbar region and medulla. There was no abnormality of the white matter. At age 50 yrs., he scored 30/40 on the Scale for the Assessment

and Rating of Ataxia (SARA), stable since at least 4 years. Sensory neuropathy with cramps and pain, square wave jerks and down beat nystagmus were noted. Deafness was evident at age 46 yrs. Because of the clinical similarity with CANVAS (sensory neuropathy, cerebellar ataxia and reduced visually enhanced vestibulo-ocular reflex), we tested for the pathological $(AAGGG)_n$ expansion in *RFC1*[2,3] but the genotype was normal (data not shown). Interestingly, his mother, an obligate carrier, was pauci-symptomatic at age 61 yrs., with slight axial instability. Follow up at age 79 yrs. revealed that she used hearing aids since at age 65 yrs. At examination, she showed head tremor and diplopia and SARA scored 4/40.

Analysis of the WES data identified a single heterozygous variant on chromosome 2 (chr2:55643155 T>C, GRCh38/hg38) that satisfied the criteria of selection and transmission, and which was absent from the gnomAD database v.2.1.1 or v.3 (https://gnomad.broadinstitute.org/). Notably, this variant lies in the region of significant linkage identified previously as SCA25 on chromosome 2 in the same family[1]. The intronic substitution is located near the canonical exon 25 splice donor site of *PNPT1* (NM_033109.5:c.2069+3 T>C). Using whole genome sequencing (WGS) performed in the affected mother-daughter pair (III-14 and IV-24), we excluded variants potentially missed by WES, and expansions in known *loci* associated with pathogenic repeats (Figure 1A; supplementary Table 1). After filtering, we identified 32 ultra-rare variants, absent from population databases and predicted to be deleterious (Combined Annotation Dependent Depletion CADD phred score[4] > 20) which were shared between the two affected individuals. The c.2069+3 T>C substitution in *PNPT1* was the only variant that mapped to SCA25 linkage region. No other candidate variant was identified from the analysis of WGS data or from an exhaustive analysis of the SCA25 chromosomal interval.

In parallel, a combined strategy including linkage, WES, WGS and RNA-Seq analysis was performed in a four-generation Australian family with ataxia and sensory neuropathy in most

affected individuals (Figure 1B). Six individuals presented with an autosomal-dominant progressive ataxia. Variable age at onset (ranging from 5 to 56 years of age) and presence of sensory neuropathy were noted, as observed in the French family. Affected individuals had diminished or absent limb reflexes, diminished sensation, and nystagmus. Cerebellar atrophy was present on MRI in those with marked ataxia. Variable penetrance of the condition was noted with the obligate carrier II-1 being unaffected at 61 years old and two other relatives (III-5 and III-7) at ages 37 and 33 respectively suffering from neuropathies but without ataxia. Linkage analyses identified four chromosomal intervals on chr.1q24.2–q25.2, 2p21–p16.1, 10p14-p13 and 15p21.3-q23, all with a peak LOD-score = 1.66, which was the maximum LOD-score achievable in this family (Figure 1C and supplementary Figure 1). The chromosome 2 linkage region identified in this family falls entirely within the SCA25 region previously identified. Combined analysis of WES and WGS and filtering of variants which segregated with the disease within the SCA25 *locus* revealed four heterozygous substitutions in the genes encoding DNA mismatch repair protein MSH6 (*MSH6*; NM_000179.2:c.2633T>C; p.Val878Ala), stonin-1 (*STON1*; NM_001198595.1:c.1231G>A; p.Glu411Lys), proteasome activator complex subunit 4 (*PSME4*; NM_014614.2:c.3400G>A; p.Glu1134Lys) and PNPT1 (*PNPT1*; NM_033109.5:c.2014-3C>G). Neither CNV nor putative pathogenic expansion within the region of linkage was detected (data not shown). Thus, *PNPT1* was retained for subsequent investigations after a comparison of results between the two large families.

Screening of *PNPT1* in a cohort of 796 French individuals with ataxia identified a frameshift variant (NM_033109.5:c.2091delA; p.Lys697AsnfsTer6) in an individual with ataxia (lower limbs) onset at 23 years. The clinical presentation included dysarthria, dystonia, sensory neuropathy, nystagmus, visual impairment, and deafness (Table 1). Segregation analysis showed that this variant was inherited from his father, who remained clinically unaffected at 86

years of age. The location of these three variants within the *PNPT1* / PNPase structure is presented on Figure 1D.

The functional effects of the variant from French families at both RNA/protein levels was assessed in primary fibroblasts. Given the proximity of the c.2069+3T>C substitution observed in family SAL-360 with the canonical splicing donor site of exon 25, a modification of *PNPT1* transcript in those with the variant was suspected. RT-PCR followed by Sanger sequencing revealed a complete skipping of exon 25 in carriers (Figure 2A). The abnormal joining of exon 24 and 26 disrupts the reading frame leading to a premature stop codon in the S1 RNA binding domain of PNPase (p.Gln672ArgfsTer18). Treatment of the cells with emetine suggested the aberrant transcript was not subject to nonsense-mediated mRNA decay (NMD). Similarly, RT-PCR followed by Sanger sequencing of the p.Lys697AsnfsTer6 variant in French family 461 similarly showed escape from NMD (Figure 2A). Western blot analysis revealed that both heterozygous variants lead to haploinsufficiency at protein level (Figure 2B). In addition, a prolonged exposure of the membrane allowed the detection of additional bands with a lower molecular weight in those with the variant, corresponding to the predicted weight of truncated proteins encoded by mutated alleles. The negligible quantity of truncated PNPase compared to the full-length protein may reflect a post-translational degradation of abnormal proteins.

Functional effects of the variant observed in the Australian family were investigated using RNA studies of a lymphoblast line established from A1-IV-2. Splice AI predicted the loss of the normal exon 25 acceptor and the gain of an acceptor at nucleotide position c.2014-4/3, resulting in a predicted frameshift and premature stop codon (p.Gln672SerfsTer6). RT-PCR followed by Sanger sequencing identified multiple transcripts at exon 25 and confirmed the effect of the variant on the RNA (Figure 2C). Similarly, RNAseq analysis revealed the abnormal transcript utilized the alternate acceptor site and accounted for approximately 10% of reads. Notably, the normalized read depth of *PNPT1* in A1-IV-2 was ~50% of the controls, strongly suggesting the

variant results in NMD of the mutant allele, with subsequent haploinsufficiency of PNPase. To confirm this, we performed western blot analysis of lymphoblasts derived from A1-IV-2 and three controls. Steady state levels of PNPase were significantly reduced in A1-IV-2 compared to the control lines (Figure 2D).

PNPT1 variations were originally associated with severe encephalomyopathy and hereditary hearing loss in bi-allelic carriers[5,6]. The mitochondrial localization of the translated protein PNPase and the association of bi-allelic variations with respiratory-chain deficiency notably lead to link mutations of *PNPT1* with mitochondrial disorders and combined oxidative phosphorylation deficiency 13 (MIM: 614932)[6]. Subsequently, functional assays to detect respiratory chain defects were performed with variable results[7–9]. Mitochondrial Oxidative Phosphorylation (OXPHOS) enzyme activities were measured using primary fibroblasts from the two brothers 360-27 (healthy non-carrier) and 360-28 (affected, heterozygous carrier) and from patient 461-7, also a heterozygous carrier. Mitochondrial respiration was not decreased in carriers of *PNPT1* variations compared with a non-carrier (supplementary Figure 2). This seems to confirm that testing for OXPHOS deficiency may not be the most appropriate way to investigate the cellular consequences of *PNPT1* pathogenic variants, as previously suggested in bi-allelic carriers[9].

More recently, bi-allelic pathogenic variants of *PNPT1* have been shown to trigger a type I interferon response linked to a defect in mtRNA processing[9–12]. Thus, we evaluated the interferon-stimulated genes (IGS) transcriptional response in peripheral blood lymphocytes (PBLs) from individuals with heterozygous variants and in controls (Figure 3A). The relative expression of six genes was used to compute an ISG score for each individual as described elsewhere (Figure 3B)[10]. ISG scores were higher in the two unrelated individuals with *PNPT1* variants compared to non-carriers. Notably, ISG values measured in affected individuals were in the same range as that previously reported in individuals with bi-allelic pathogenic variants

in *PNPT1*[9,10,12]. The ISG score for the unaffected individual with a pathogenic *PNPT1* variant was close to the score measured in non-carrier (control) individuals. The same trend between carriers and non-carriers was observed in a second experiment performed with independent PBLs collected at a different age at sampling for individuals with a pathogenic variant (supplementary Figure 3 and supplementary table 2).

The genetic basis of the SCA25 locus had eluded discovery since the disorder was first mapped in 2004. In this study we report converging data from two large families with autosomal dominant spinocerebellar ataxia that map to the SCA25 *locus*. NGS performed in these two families combined with linkage analyses identified nonsense variants, either splice or frameshift, in *PNPT1*. An exhaustive search for *PNPT1* variants in a cohort of individuals with SCA led to the detection of only one additional individual with a nonsense variant. Bi-allelic pathogenic variants in *PNPT1* have been previously associated with variable diseases ranging from non-syndromic hearing loss to multisystemic Leigh disease, and with other clinical conditions manifesting visual defects, abnormal muscle tone, speech delays, feeding difficulties, scoliosis and/or sensory neuropathy[5,6,8,9,11,13–15]. These previously described clinical conditions were all observed in families with a recessive model of inheritance. Many of these symptoms are overlapping with the clinical presentation of the individuals we have identified with heterozygous *PNPT1* variants. However, the majority of symptoms described in individuals with bi-allelic pathogenic variants appeared in the first year of life, in contrast to those with a heterozygous variant, in whom symptoms appeared at ages ranging from 17 months through to incomplete penetrance at age 86 for the oldest healthy carrier[1,9,12]. This suggests that penetrance may be lower, and expressivity more variable in individuals with heterozygous variants. In these previous studies describing bi-allelic variants in *PNPT1*, very little information was available regarding the heterozygous parents suggesting that they were healthy at the time of publication. An alternative explanation for the apparent lack of clinical

presentation in heterozygous carriers of pathogenic bi-allelic variants could be the location of the variants, resulting in a possible genotype-phenotype correlation for the risk of developing ataxia (Figure 1D). The three loss-of-function variants described in our study, indicated below the protein schematic, are all located in the S1-domain. Strikingly, two of them alter the protein sequence from the same amino-acid position and all induce a premature stop in the S1-domain. In contrast, previous studies demonstrate pathogenic bi-allelic variants, indicated above the protein schematic (Figure 1D), are located throughout the gene. Only two previous reports described patients who developed ataxia in adulthood. As shown in Figure 1D, both of these patients had missense variants within the S1-domain[9,15]. Thus, it is reasonable to speculate that variants affecting the S1 domain may be associated with ataxia and nonsense variations in this domain may predispose to the development of ataxia in heterozygous carriers. This domain plays a crucial role in RNA binding. Thus, variants affecting the S1-domain, which reduce the expression of PNPase and / or which lead to proteins lacking this domain, as we observed in immunoblots, may alter or destabilize the homotrimeric structure of the enzyme, and this mechanism, through a dominant-negative effect, might be the basis of the genotype-phenotype correlation.

The protein PNPase is located in both the mitochondrial matrix and the intermembrane space[5,6,14]. This exoribonuclease is reported to play a dual role in RNA import into the mitochondria, and in preventing the accumulation of double-stranded mtRNAs in mitochondria[5,6,10,14]. Notably, individuals with bi-allelic hypomorphic variants in this gene display mitochondrial double-stranded RNA accumulation with a subsequent leakage into the cytosol leading to aberrant type I interferon activation[10]. In our series the ISG scores were higher in affected heterozygous carriers compared with non-carriers, suggesting that the same triggering of a type I interferon response occurs in individuals with both bi-allelic and heterozygous variants in this gene. This aberrant response may also directly result in the

development of disease. An increased IFN activation may drive neuroinflammation leading to neuronal dysfunction and/or neuronal loss. However, our present study cannot definitively determine if this activation is involved in the pathogenesis, or alternatively a biological marker of the disease. Interestingly, the ISG score in the heterozygous carrier still healthy at age 86 was close to the values measured in non-carriers. This result suggests that the limitation of an elevated type I interferon response may directly or indirectly prevent deleterious effects of pathogenic *PNPT1* variations. A variable type I interferon response among carriers may also explain the striking intrafamilial variability observed in SCA25.

To conclude, our work not only describes *PNPT1* as the SCA25 gene, but also establishes a link between SCA25 and Mendelian type I interferonopathies suggesting a common pathological pathway. How the alteration of mtRNA trafficking and the subsequent aberrant type I interferon response caused by *PNPT1* haploinsufficiency is associated with cerebellar dysfunctions remains to be explained.

Data and code availability

This study did not generate datasets or code.

Supplemental information

Supplemental information (supplemental material and method, supplemental figures and tables) can be found online at XXX.

Acknowledgments

Part of this work was carried out on the iGenSeq sequencing and the Data Analysis Core bioinformatic facilities of the ICM. The authors would like to thank Michael Wilson, Greta Gillies and Kate Pope (Murdoch Children's Research Institute) for their technical assistance. We thank the patients and their families for participation in this study.

Declaration of interests

no conflict of interest.

Web resources

CADD, https://cadd.gs.washington.edu

gnomAD, https://gnomad.broadinstitute.org

Online Mendelian Inheritance in Man, https://www.omim.org/

Funding

The research leading to these results has received funding from the program “Investissements d’avenir” ANR-10- IAIHU-06 and ANR-11- INBS-0011 – NeurATRIS: Translational Research Infrastructure for Biotherapies in Neurosciences. European funding: 6th PCRD (EUROSCA, to AB), 7th PCRD (Neuromics, to AB) et H2020 (SOLVE-RD, to GS) ; Agence Nationale de la recherche (ANR SPATAX-QUEST, to GS), Association Connaitre les syndromes cérébelleux (to GS) and Fondation Maladies Rares (to GS).

Australian National Health and Medical Research Council (NHMRC) Senior Research Fellowship (1102971) to M.B. KCD was supported by an Australian Postgraduate Award. R.M.T. was supported by an Australian Postgraduate Award and funding from the Edith Moffat fund. BREA was supported by an NHMRC Early Career Fellowship (1157776). PJL was funded by the Vincent Chiodo Foundation and this work was supported in part by NHMRC GNT2001513 to PJL and MBD. Additional funding was provided by the Independent Research Institute Infrastructure Support Scheme and the Victorian State Government Operational Infrastructure Program. Italian Ministry for Education, University and Research (Ministero dell’Istruzione, dell’Università e della Ricerca - MIUR) under the programme “Dipartimenti di Eccellenza 2018 – 2022” Project code D15D18000410001 to AB.

Figure legends

Figure 1. Pedigrees of families with autosomal dominant spinocerebellar ataxia mapping to the SCA25 *locus*. (**A**): Pedigree of the French family (AAD-360). (**B**): Pedigree of the A1 Australian family. Orange symbols indicate family members heterozygous for pathogenic variants in *PNPT1*. Black arrows indicate probands. DNA from circled individuals was used

for whole-exome sequencing (dotted lines) or whole-genome sequencing (solid lines). (**C**) Multipoint LOD scores from parametric linkage analyses performed in the A1 family across the chromosome 2. The blue area corresponds to the SCA25 *locus* mapped previously in the French family AAD-360. (**D**) Lollipop plot and exon map depicting the distribution of pathogenic variants in the polynucleotide phosphorylase (PNPase) protein. Bi-allelic variants previously described in the literature are shown above the protein schematic. Heterozygous variants identified in this study are shown below. Variants reported in individuals with ataxia are marked by the asterisk. All reported individuals with bi-allelic variants that present with ataxia are compound heterozygotes. Each pair of variants in an individual with ataxia is marked with a different color #. RNase_PH = 3' exoribonuclease family, domain 1; Rnase_PH_C = 3' exoribonuclease family, domain 2; PNPase = Polyribonucleotide nucleotidyltransferase, RNA binding domain; KH_1 = KH domain; S1 = S1 RNA binding domain.

Figure 2. *PNPT1* variants alter transcripts and PNPase protein levels. (**A**): Analysis of *PNPT1* transcripts from fibroblasts cultured with or without emetine in two patients (360-28 and 461-7) *vs*. a non-carrier (360-27). Alterations of the wild-type sequence of the transcript are indicated. (**B**): Immunoblots of PNPase in the corresponding fibroblasts. Bands corresponding to PNPase are shown with two different time of exposure (the longer being below). Quantitation of signal intensities from two independent blots is presented on the right panel. The steady state level of PNPase in the untreated control fibroblasts (360-27) has been adjusted to 100% and the other samples normalized to this result, showing significant reduction in affected carriers compared to control. (**C**): Analysis of *PNPT1* transcripts from lymphoblast cells from A1-IV-2. Sanger sequence of RT-PCR products spanning exon 24 to 26 identified an aberrant transcript, which was confirmed by RNAseq analysis. The relative expression level of *PNPT1* suggested the mutant allele was being degraded by NMD. (**D**): Western blot analysis

suggested a decrease in steady state PNPase levels in patient-derived lymphoblasts cells and quantitation of three independent blots confirmed a significant reduction compared to control.

Figure 3. Activation of interferon-stimulated genes (ISGs) in affected individuals with heterozygous variations of *PNPT1*. (**A**) Aggregate ISG scores in blood: individual value of ISG score in PBLs of non-carriers (open bar), one healthy carrier (grey bar) and two patients (black bars). ISG values from three patients with homozygous variations of *PNPT1* (marked with an asterisk, striped bars) published already published by Dhir et *al*. have been added for comparison. (**B**) RT–qPCR analysis of the six individual genes that make up the aggregate ISGs in whole blood from non-carriers 461-2 and 360-27 (open bars), asymptomatic carrier 461-3 (grey bars) and patients 461-7 and 360-28 (black bars). The data plotted (mean and SD from duplicates) is relative quantification (RQ) values for each gene per patient.

References

1. Stevanin, G., Bouslam, N., Thobois, S., Azzedine, H., Ravaux, L., Boland, A., Schalling, M., Broussolle, E., Dürr, A., and Brice, A. (2004). Spinocerebellar ataxia with sensory neuropathy (SCA25) maps to chromosome 2p. Ann Neurol *55*, 97–104.

2. Cortese, A., Simone, R., Sullivan, R., Vandrovcova, J., Tariq, H., Yau, W.Y., Humphrey, J., Jaunmuktane, Z., Sivakumar, P., Polke, J., et al. (2019). Biallelic expansion of an intronic repeat in RFC1 is a common cause of late-onset ataxia. Nat. Genet. *51*, 649–658.

3. Rafehi, H., Szmulewicz, D.J., Bennett, M.F., Sobreira, N.L.M., Pope, K., Smith, K.R., Gillies, G., Diakumis, P., Dolzhenko, E., Eberle, M.A., et al. (2019). Bioinformatics-Based Identification of Expanded Repeats: A Non-reference Intronic Pentamer Expansion in RFC1 Causes CANVAS. Am J Hum Genet *105*, 151–165.

4. Kircher, M., Witten, D.M., Jain, P., O'Roak, B.J., Cooper, G.M., and Shendure, J. (2014). A general framework for estimating the relative pathogenicity of human genetic variants. Nat. Genet. *46*, 310–315.

5. von Ameln, S., Wang, G., Boulouiz, R., Rutherford, M.A., Smith, G.M., Li, Y., Pogoda, H.-M., Nürnberg, G., Stiller, B., Volk, A.E., et al. (2012). A mutation in PNPT1, encoding mitochondrial-RNA-import protein PNPase, causes hereditary hearing loss. Am J Hum Genet *91*, 919–927.

6. Vedrenne, V., Gowher, A., De Lonlay, P., Nitschke, P., Serre, V., Boddaert, N., Altuzarra, C., Mager-Heckel, A.-M., Chretien, F., Entelis, N., et al. (2012). Mutation in PNPT1, which encodes a polyribonucleotide nucleotidyltransferase, impairs RNA import into mitochondria and causes respiratory-chain deficiency. Am J Hum Genet *91*, 912–918.

7. Matilainen, S., Carroll, C.J., Richter, U., Euro, L., Pohjanpelto, M., Paetau, A., Isohanni, P., and Suomalainen, A. (2017). Defective mitochondrial RNA processing due to PNPT1 variants causes Leigh syndrome. Hum Mol Genet *26*, 3352–3361.

8. Alodaib, A., Sobreira, N., Gold, W.A., Riley, L.G., Van Bergen, N.J., Wilson, M.J., Bennetts, B., Thorburn, D.R., Boehm, C., and Christodoulou, J. (2016). Whole-exome sequencing identifies novel variants in PNPT1 causing oxidative phosphorylation defects and severe multisystem disease. Eur J Hum Genet *25*, 79–84.

9. Rius, R., Van Bergen, N.J., Compton, A.G., Riley, L.G., Kava, M.P., Balasubramaniam, S., Amor, D.J., Fanjul-Fernandez, M., Cowley, M.J., Fahey, M.C., et al. (2019). Clinical Spectrum and Functional Consequences Associated with Bi-Allelic Pathogenic PNPT1 Variants. J Clin Med *8*,.

10. Dhir, A., Dhir, S., Borowski, L.S., Jimenez, L., Teitell, M., Rötig, A., Crow, Y.J., Rice, G.I., Duffy, D., Tamby, C., et al. (2018). Mitochondrial double-stranded RNA triggers antiviral signalling in humans. Nature *560*, 238–242.

11. Bamborschke, D., Kreutzer, M., Koy, A., Koerber, F., Lucas, N., Huenseler, C., Herkenrath, P., Lee-Kirsch, M.A., and Cirak, S. (2021). PNPT1 mutations may cause Aicardi-Goutières-Syndrome. Brain Dev *43*, 320–324.

12. Pennisi, A., Rötig, A., Roux, C.-J., Lévy, R., Henneke, M., Gärtner, J., Teke Kisa, P., Sarioglu, F.C., Yiş, U., Konczal, L.L., et al. (2020). Heterogeneity of PNPT1 neuroimaging: mitochondriopathy, interferonopathy or both? J Med Genet.

13. Slavotinek, A.M., Garcia, S.T., Chandratillake, G., Bardakjian, T., Ullah, E., Wu, D., Umeda, K., Lao, R., Tang, P.L.-F., Wan, E., et al. (2015). Exome sequencing in 32 patients with anophthalmia/microphthalmia and developmental eye defects. Clin Genet *88*, 468–473.

14. Sato, R., Arai-Ichinoi, N., Kikuchi, A., Matsuhashi, T., Numata-Uematsu, Y., Uematsu, M., Fujii, Y., Murayama, K., Ohtake, A., Abe, T., et al. (2018). Novel biallelic mutations in the PNPT1 gene encoding a mitochondrial-RNA-import protein PNPase cause delayed myelination. Clin Genet *93*, 242–247.

15. Eaton, A., Bernier, F.P., Goedhart, C., Caluseriu, O., Lamont, R.E., Boycott, K.M., Parboosingh, J.S., Innes, A.M., and Care4Rare Canada Consortium (2018). Is PNPT1-related hearing loss ever non-syndromic? Whole exome sequencing of adult siblings expands the natural history of PNPT1-related disorders. Am J Med Genet A *176*, 2487–2493.

Table

Table 1. Clinical features of affected individuals with *PNPT1* variations from the French index cases from family 360 (all relatives extensively described in Stevanin *et al*. 2004) and family 461, and carriers from the Australian family A1.

Patient	Age at exam	Age at onset	Predominant sign (handicap/7)	Cerebellar ataxia score (SARA)	Ocular signs	Reflexes (plantar reflexe)	Vibration sense at ankles	Urinary symptoms	Hearing loss	Cognitive impairment	ENMG	Brain MRI	Additional signs
360-28 (index)	22	17mo	Sensory and cerebellar ataxia (6)	Severe	Square waves jerks, nystagmus hypermetric	Absent (flexor)	Abolished	none	yes	none	Sensory neuronopathy	ND	Scoliosis, facial tics, vomiting, pas cavus, wasting
	32	17mo	Sensory and cerebellar ataxia (6)	Severe	Square waves jerks, nystagmus hypermetric	Absent (flexor)	Abolished	none	yes	none		Cerebellar atrophy	Cough
	50	17mo	Sensory and cerebellar ataxia (6)	Severe (30/40)	Down beat nystagmus	Absent (unilateral extensor)	Abolished	none	deafness	none		Cerebellar and bulbar atrophy, periventricular white matter changes	Cramps
461-7 (index)	40	23	Ataxia (6)	Moderate (24/40)	Nystagmus and slow saccades	Absent (flexor)	Abolished	None	Deafness	None	Sensory neuronopathy, mild myopathy	Cerebellar atrophy periventricular white matter changes	

A1-II-3	58	21	Wheelchair for mobility, moderate cerebellar dysarthria, , gross upper and lower limb ataxia,	impaired vestibulo-ocular reflex gain, gaze-evoked horizontal nystagmus, mild vertical nystagmus, hypermetric saccades	Absent reflexes in upper and lower limbs, extensor plantar responses				Cerebellar atrophy	Pes cavus, claw toes, diminished sensation in feet
A1-II-1	56	56	Very subtle incoordination		Normal					Normal sensation
A1-III-1 (index)	20	10	Ambulant, with upper and lower limb ataxia	Restriction of upper and lateral gaze, no nystagmus	Absent reflexes and equivocal plantar responses	Reduced			Cerebellar atrophy	
A1-III-2	21	20	Minimal gait ataxia, mild finger-nose ataxia, no dysarthria	No nystagmus	Absent reflexes, extensor plantar responses				Cerebellar atrophy	
A1-III-5	37		none		Reduced reflexes			Sensory neuropathy	Normal	
A1-III-7	33		none					Axonal sensory neuropathy with mild axonal motor neuropathy		
A1-IV-1	6	5	Unable to tandem walk, positive Romberg sign	Nystagmus	Absent reflexes			Sensory neuropathy	Cerebellar atrophy	

A1-IV-2	6	5	Required K-walker		Absent reflexes			Sensory neuropathy	Cerebellar atrophy
A1-IV-3	6	9	Required K-walker, severer dysarthria	Mild nystagmus, dysmetria, oculomotor apraxia	Absent knee jerks and reduced ankle jerks				Moderate to severe cerebellar hemisphere and vermian atrophy, normal brainstem

Figure

Figure 1.

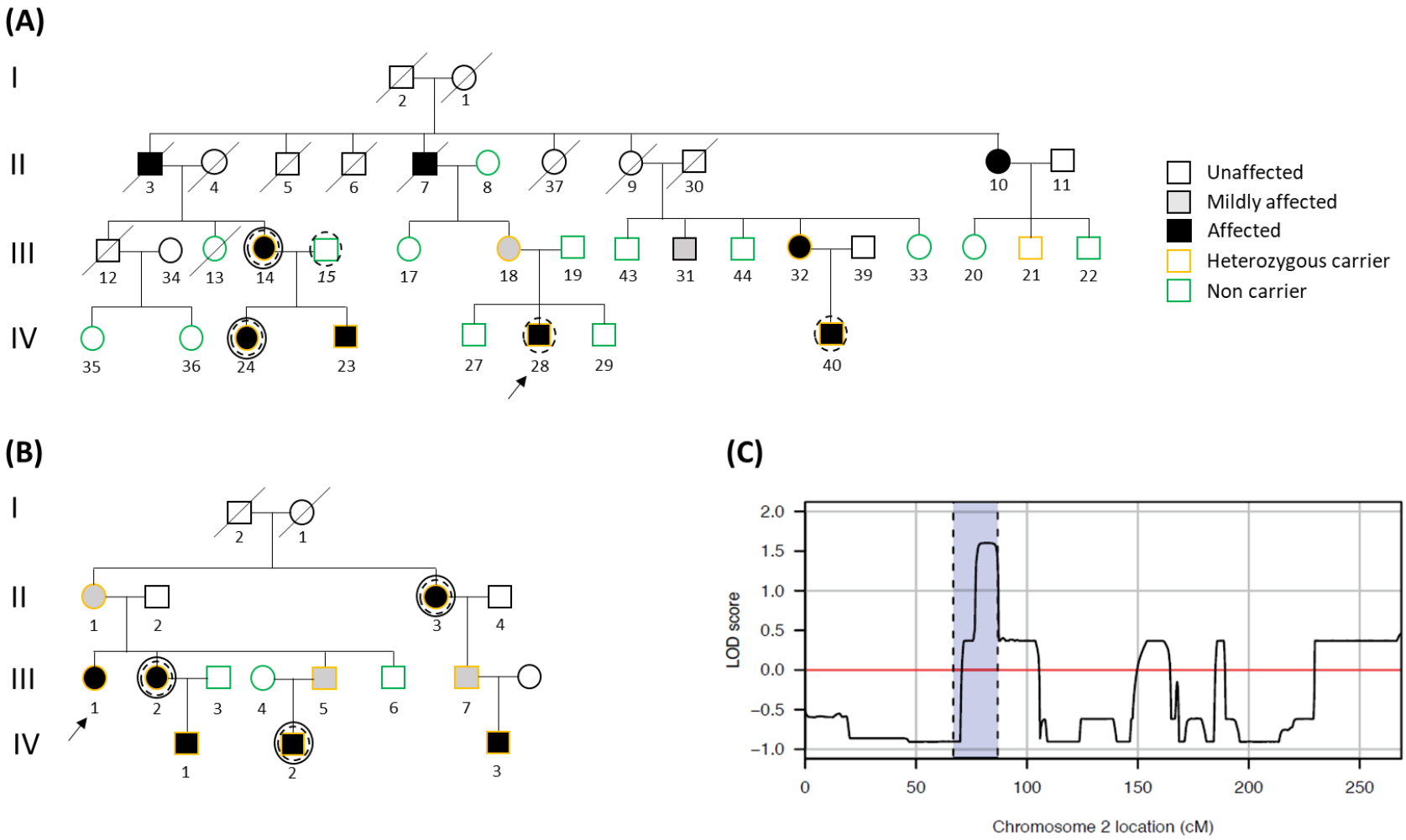

(D)

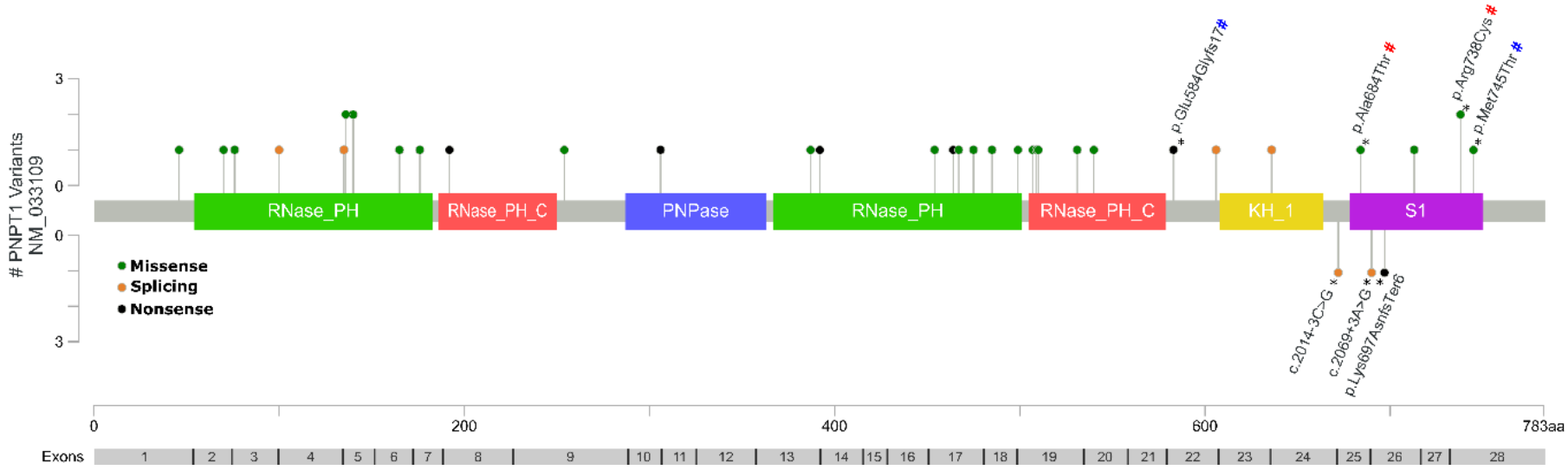
PNPT1 Variants
NM_033109
3
0
0
3
Missense
Splicing
Nonsense
RNase_PH
RNase_PH_C
PNPase
RNase_PH
RNase_PH_C
KH_1
S1
p.Glu584Glyfs17*
p.Ala684Thr
p.Arg738Cys
p.Met745Thr
c.2014-3C>G
c.2069+3A>G
p.Lys697Asnfs*6
0
200
400
600
783aa
Exons
1
2
3
4
5
6
7
8
9
10
11
12
13
14
15
16
17
18
19
20
21
22
23
24
25
26
27
28

Figure 2.

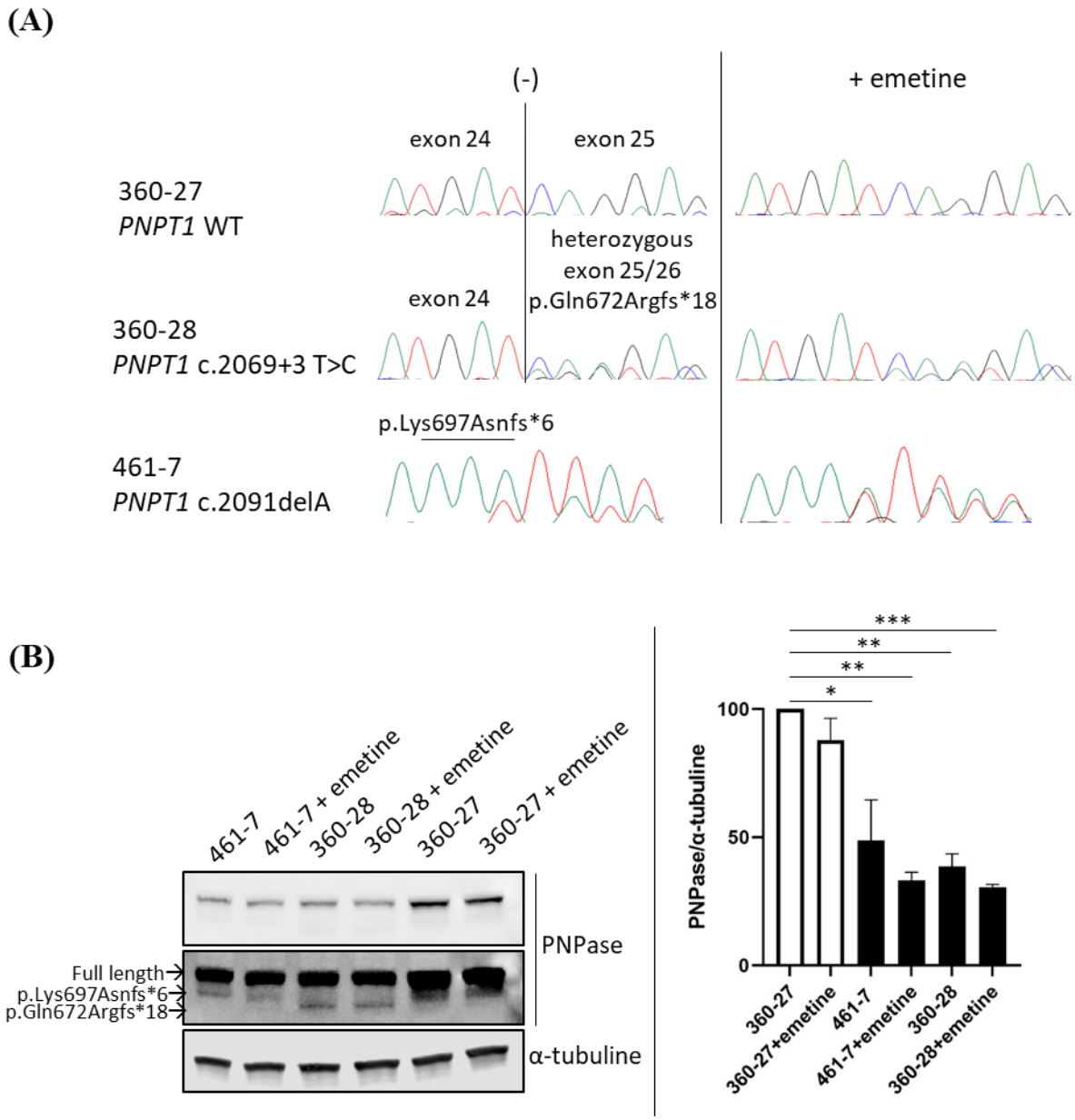
(A)
(-)
+ emetine
exon 24
exon 25
360-27
PNPT1 WT
heterozygous
exon 25/26
p.Gln672Argfs*18
exon 24
360-28
PNPT1 c.2069+3 T>C
p.Lys697Asnfs*6
461-7
PNPT1 c.2091delA
(B)
461-7
461-7 + emetine
360-28
360-28 + emetine
360-27
360-27 + emetine
Full length
p.Lys697Asnfs*6
p.Gln672Argfs*18
PNPase
α-tubuline
PNPase/α-tubuline
100
50
0
***
**
**
*
360-27
360-27+emetine
461-7
461-7+emetine
360-28
360-28+emetine

(C)

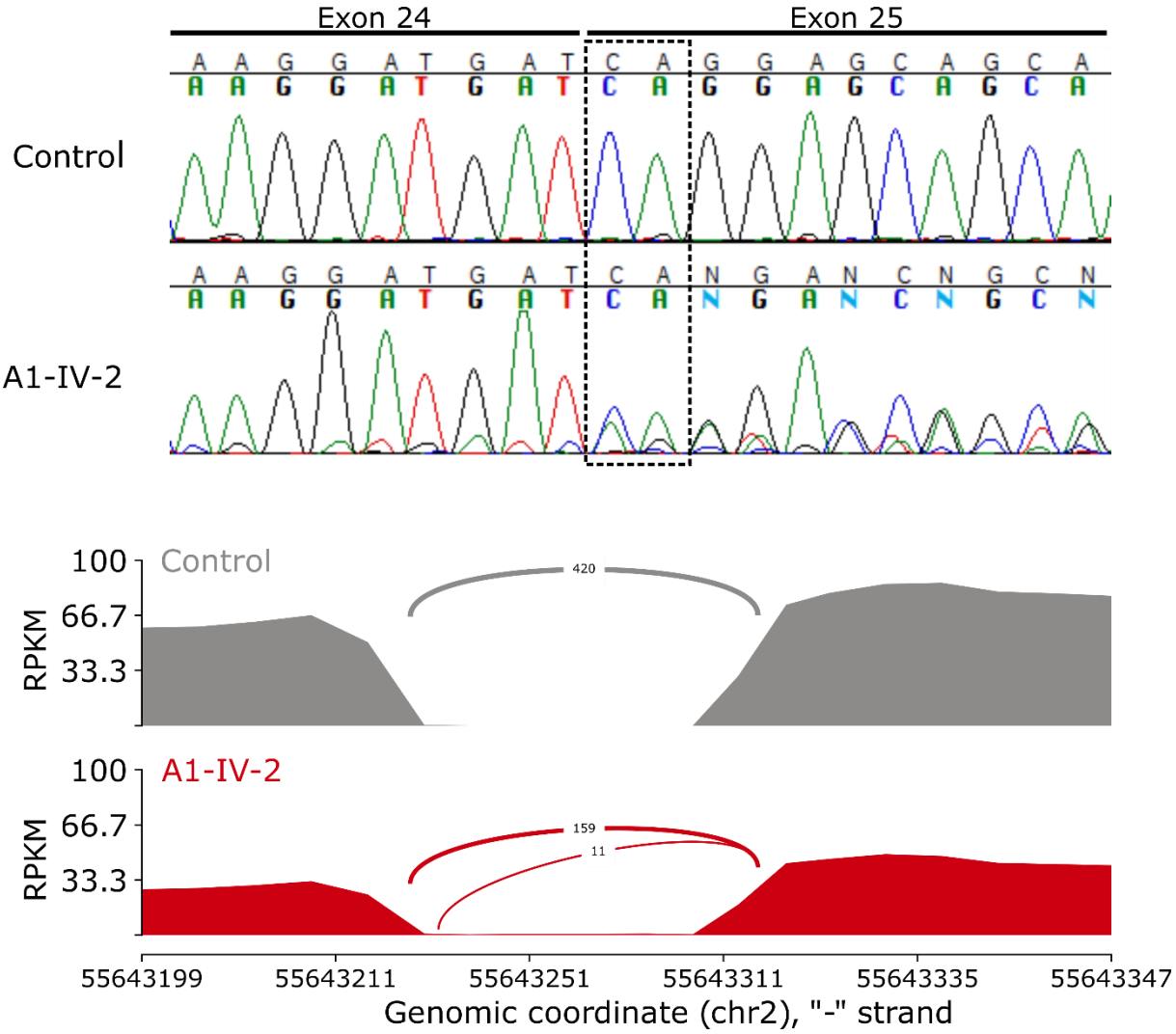
Exon 24
Exon 25
Control
A1-IV-2
100
66.7
33.3
RPKM
Control
420
A1-IV-2
159
11
55643199
55643211
55643251
55643311
55643335
55643347
Genomic coordinate (chr2), "-" strand

(D)

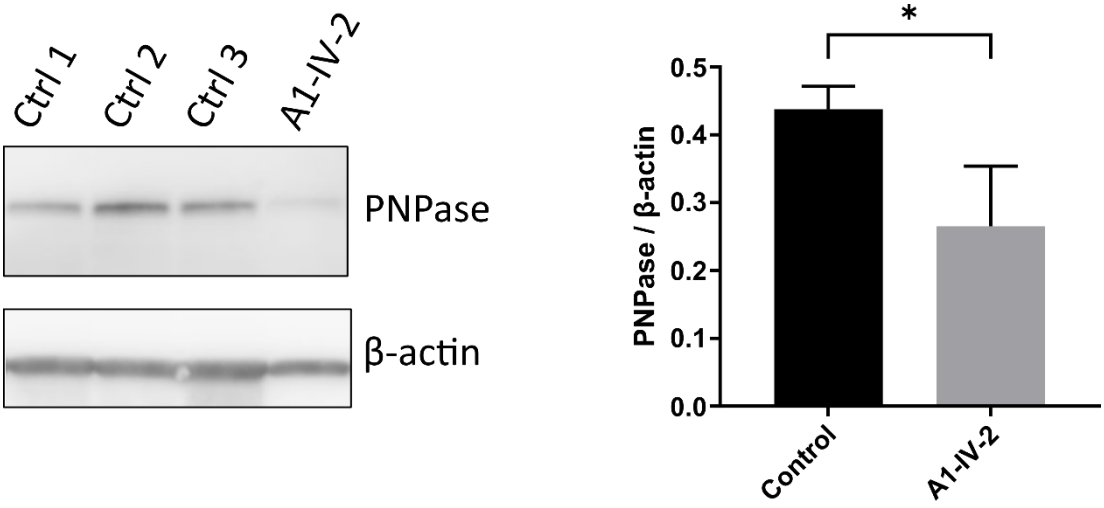
Ctrl 1
Ctrl 2
Ctrl 3
A1-IV-2
PNPase
β-actin
*
PNPase / β-actin
0.5
0.4
0.3
0.2
0.1
0.0
Control
A1-IV-2

Figure 3.

(A)

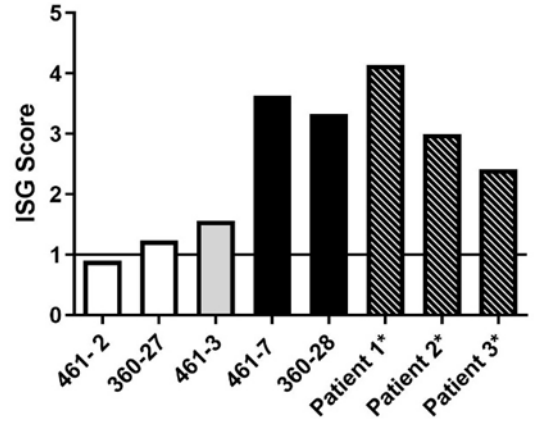
ISG Score
5
4
3
2
1
0
461- 2
360-27
461-3
461-7
360-28
Patient 1*
Patient 2*
Patient 3*

(B)

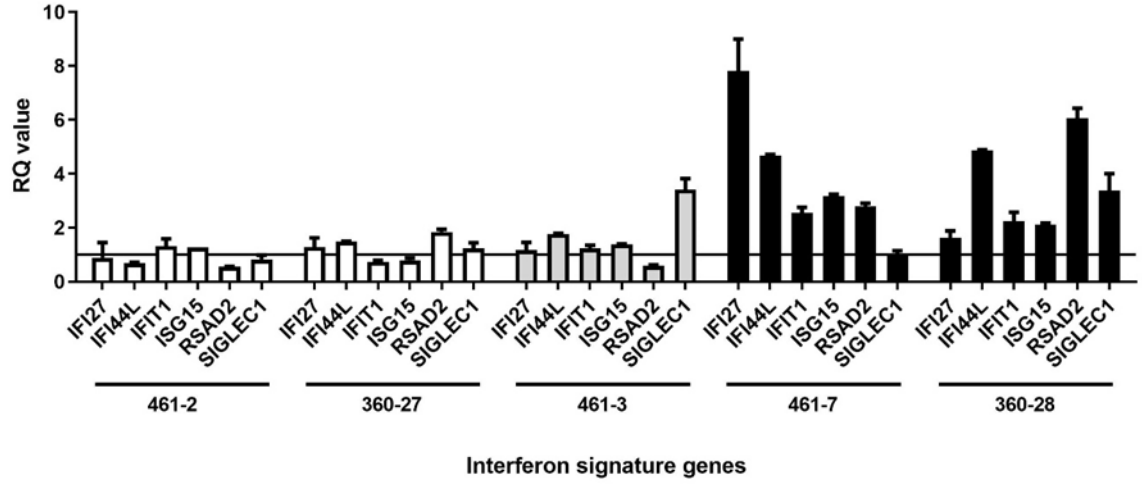
RQ value
10
8
6
4
2
0
IFI27
IFI44L
IFIT1
ISG15
RSAD2
SIGLEC1
461-2
360-27
461-3
461-7
360-28
Interferon signature genes